UNITED NATIONS EDUCATIONAL, SCIENTIFIC AND CULTURAL ORGANIZATION
INTERNATIONAL ATOMIC ENERGY AGENCY
INTERNATIONAL CENTRE FOR THEORETICAL PHYSICS
I.C.T.P., P.O. BOX 586, 34100 TRIESTE, ITALY, CABLE: CENTRATOM TRIESTE

SMR.998d - 22

Research Workshop on Condensed Matter Physics
30 June - 22 August 1997
MINIWORKSHOP ON
QUANTUM WELLS, DOTS, WIRES
AND SELF-ORGANIZING NANOSTRUCTURES
11 - 22 AUGUST 1997

"Electronic Structure and Optical Properties of GaAs Quantum Wells Embedded in AlAs/GaAs Superlattices"

V.T. DONCHEV
University of Sofia
Department of Condensed Matter Physics
Faculty of Physics
5 Boulevard James Bouchier
BG-1164 Sofia
BULGARIA

These are preliminary lecture notes, intended only for distribution to participants.

ELECTRONIC STRUCTURE AND OPTICAL PROPERTIES OF GaAs QUANTUM WELLS EMBEDDED IN ALAS/GAAS SUPERLATTICES

V. DONCHEV

Dept. of Condensed Matter Physics, Faculty of Physics, Sofia University,

S. VLAEV

Institute of General and Inorganic Chemistry, Bulgarian Academy of Sciences

I. IVANOV

Dept. of Physics and Measurement Technology, Linköping University, Sweden

K. GERMANOVA

Dept. of Solid State Physics and Microelectronics, Faculty of Physics,
Sofia University,

I. Introduction

Quantum heterostructures GaAs/AlGaAs have been extensively studied because of their multiple applications due to the very close lattice constants of GaAs and AlAs [1]. Usually one considers GaAs quantum wells (QWs) with barriers of AlAs or AlGaAs and unperturbed superlattices (SLs) with good periodicity.

Less numerous are the works which investigate GaAs QWs having SLs as barrier layers. Such systems are called also

- QWs embedded in a SL or
- SLs with enlarged QWs.

They are very interesting from both theoretical and practical point of view because:

1. They show interesting physical properties [2,3];
2. The use of SL structures as prelayers suppress the defect diffusion from the substrate to the QW and relieves the strain caused by the small lattice mismatch between GaAs and AlAs, thus improving the device performance [4,5];
3. The presence of SLs allows a better control of the system structural parameters which is important especially in the case of growth on patterned substrates.
4. SLs with an enlarged well (EW) are used for study of carrier transport perpendicular to the SL layers [6]

The aim of this work is to present some results on GaAs QW embedded in short period AlAs/GaAs SLs obtained in our research team. It includes:

1. results of theoretical calculations of the electronic structure of these systems;
2. experimental results obtained by PL spectroscopy;
3. an attempt to explain the experimental observations by means of the theoretical calculations.

II. Theoretical calculations of the electronic structure

i) structures considered

The structures considered are schematically represented on Fig.1. They consist in a GaAs QW embedded in an AlAs(4)/GaAs(8) SL (20.5 periods of both sides) which is surrounded by semi-infinite uniform regions of $Al_xGa_{1-x}As$ with x equal to the mean Al content in the SL.

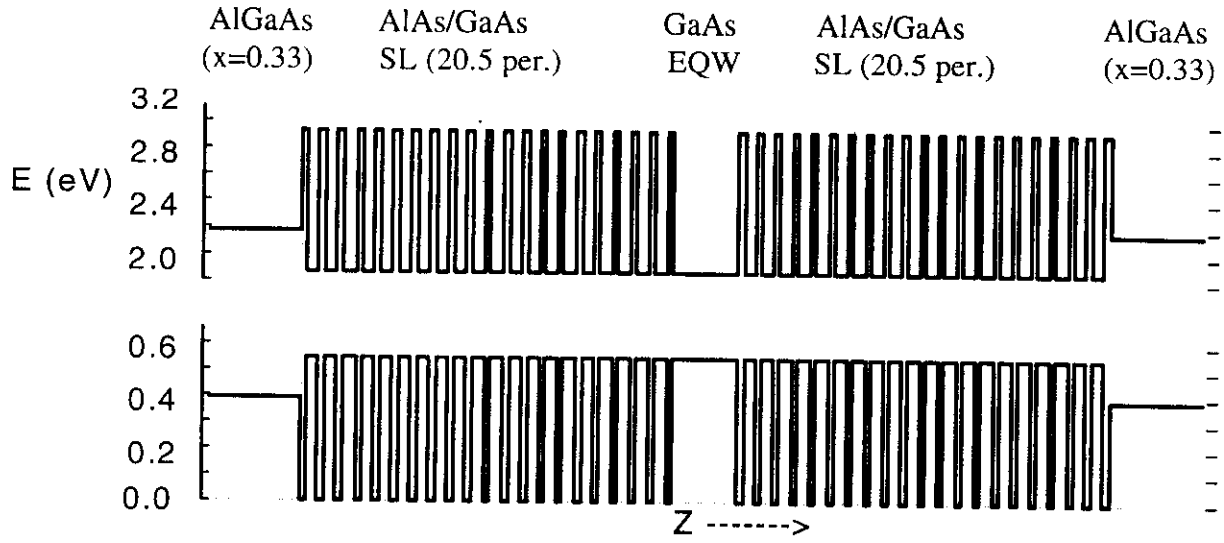

Figure 1. Structures considered in the calculations

ii) *method of calculations*

The calculations are performed using the tight-binding approach. They are based on a semi-empirical tight-binding Hamiltonian matrix describing a nearest-neighbor model in a basis with 5 orbitals (s, p_x ,p_y , p_z , s^*), which has been proved useful in practice. The tight-binding parameters are taken from the literature [7,8] The zero energy level is at the Γ point of the AlAs valence band. A band offset ratio of 66 / 34 has been used. The AlGaAs has been treated in the VCA (virtual crystal approximation) and his TB parameters are taken as a linear combination of the TB parameters of GaAs and AlAs: $TBP(Al_xGa_{1-x}) = x*TBP(AlAs) + (1-x)*TBP(GaAs)$.

The method of the Green functions is used. The density of states (DOS) is found from the imaginary part of the Green function. To find the Green function of the system the SGFM (surface Green function matching) formalism [9] is employed. The system is consider as formed by one nonhomogeneous region surrounded by 2 semi-infinite homogeneous regions. In our case the nonhomogeneous region is the EW plus the SL, and the homogeneous regions are the AlGaAs regions. The total Green function matrix is a function of the Green functions of the three regions.

G_1	G_2	G_3
homogen.	NONhomog.	homogen.

G_1 and G_3 are calculated by means of the transfer matrices method while an original algorithm (already established and used to study other heterogeneous structures [10-12]) has been used to find the Green function G_2 of the nonhomogeneous region. The algorithm used for the semi-empirical numerical calculations can be found in [10]. The calculations are done for the Γ point of the two-

dimensional Brillouin zone in (001) direction. From the energy dependence of the DOS we find the energies of electrons and holes. Heavy holes and light holes can be distinguished bearing in mind that the P_z orbitals of hh have very low (nearly zero) amplitude, while for lh they are larger that the P_x and P_y orbitals. Dependencies of the spectral strength as a function of the Z - direction are also calculated. For comparison we have considered also GaAs/ $Al_xGa_{1-x}As$ single quantum wells (SQWs) with x=0.33 and x=1. The first value corresponds to the mean Al content in the SL, while the second one - to the barriers of the SL.

iii) *Electron and hole energies*

Table 1.Electron and hole energies (**ETB** calculations)

GaAs QW of 18 monolayers		GaAs QW of 42 monolayers	
SQW GaAs /AlGaAs x=0.33 x=1	GaAs QW embedded in an AlAs(4)/GaAs(8) SL	SQW GaAs/AlGaAs x=0.33 x=1	GaAs QW embedded in an AlAs(4)/GaAs(8) SL
2285 (e2) 2330	2336 (EW, SL)	2295 (e4) 2317	2320 (EW,SL)
	2264 - 2316 (SL,EW)		*2264-2316(SL,EW)*
2151 (e1) 2163	2163 (e1) (EW)	2218 (e3) 2230 2154 (e2) 2160 2113 (e1) 2114	2229 (EW) 2160 EW) 2114 (e1) (EW)
gap		gap	
527 (hh1) 522 503 (lh1) 490	522 (hh1) (EW) 490 (lh1) (EW)	543 (hh1) 542 534 (lh1) 532 527 (hh2) 525 502 (hh3) 497 496 (lh2) 488 468 (hh4) 459	542 (hh1) (EW) 532 (lh1) (EW) 525 (hh2) (EW) 497 (hh3) (EW) 488 (lh2) (EW) 459 (hh4) (EW, SL)
	461 - 451 (SL, EW)		*461 - 451 (SL, EW)*
467 (hh2) 446	446 (hh) (EW, SL)	440 (lh3) 423	428 (lh3) (EW,SL))
	423 - 350 (SL, EW)		*423 - 350 (SL, EW)*
(lh2) 344 399 (hh3) 329	335 (lh) (EW, SL) 328 (hh) (EW, SL)	426 (hh5) 411 381 (hh6) 354 (lh4?) 347	411 (hh) (EW, SL) 354 (EW, SL) 342 (EW, SL)

Table 1 represents the electron and holes energies for two GaAs QWs - of 18 and 42 monolayers, respectively. These widths correspond to the widths of the EWs in the samples studied

experimentally. Three cases are considered, namely SQW with AlGaAs (x=0.33) barriers, SQW with AlAs barriers and QW embedded in an AlAs/GaAs SL with 4 an 8 MLs of AlAs and GaAs, respectively. The type of the states and their localization (in the case of EW) are given in parentheses. The zero energy level is at the top of the AlAs valence band.

As expected, when the AlGaAs barrier is replaced by AlAs, the energies of all the states of the SQW increase (if measured from the bottom of the wells). This way they approaches the energies of the EW.

Further on the lowest electron, heavy hole and light hole states of the EW have the same energies as the corresponding states in the GaAs/AlAs SQW. Besides, they are localized predominantly in the EW similarly to the states of the SQW. Note that the energies of these states are far away from the SL mini-bands.

The energy of the 4th electron state of the GaAs/AlAs SQW (2317meV) is close to the SL mini-band (2264-2316meV). The corresponding EW state is shifted to higher energies by 3meV ((e4)=2320meV), but still remains close to the mini-band. Its wave function shows 4 maxima in the EW similarly to the case of SQW. However a substantial delocalization in the SL is also present (Fig.2). On the other hand some SL states penetrate in the EW revealing also 4 maxima (Fig.2, right side). The situation s similar for the states hh4 and lh3 of the same EW and the states (e2), (hh2) and (lh2) of the EW of 18 MLs (Fig.3). Note that they all are close or inside a SL mini-band. So, an interaction between the EW and the SL is observed. It is connected to the fact that the state coming from the EW has an energy close to the SL mini-band.

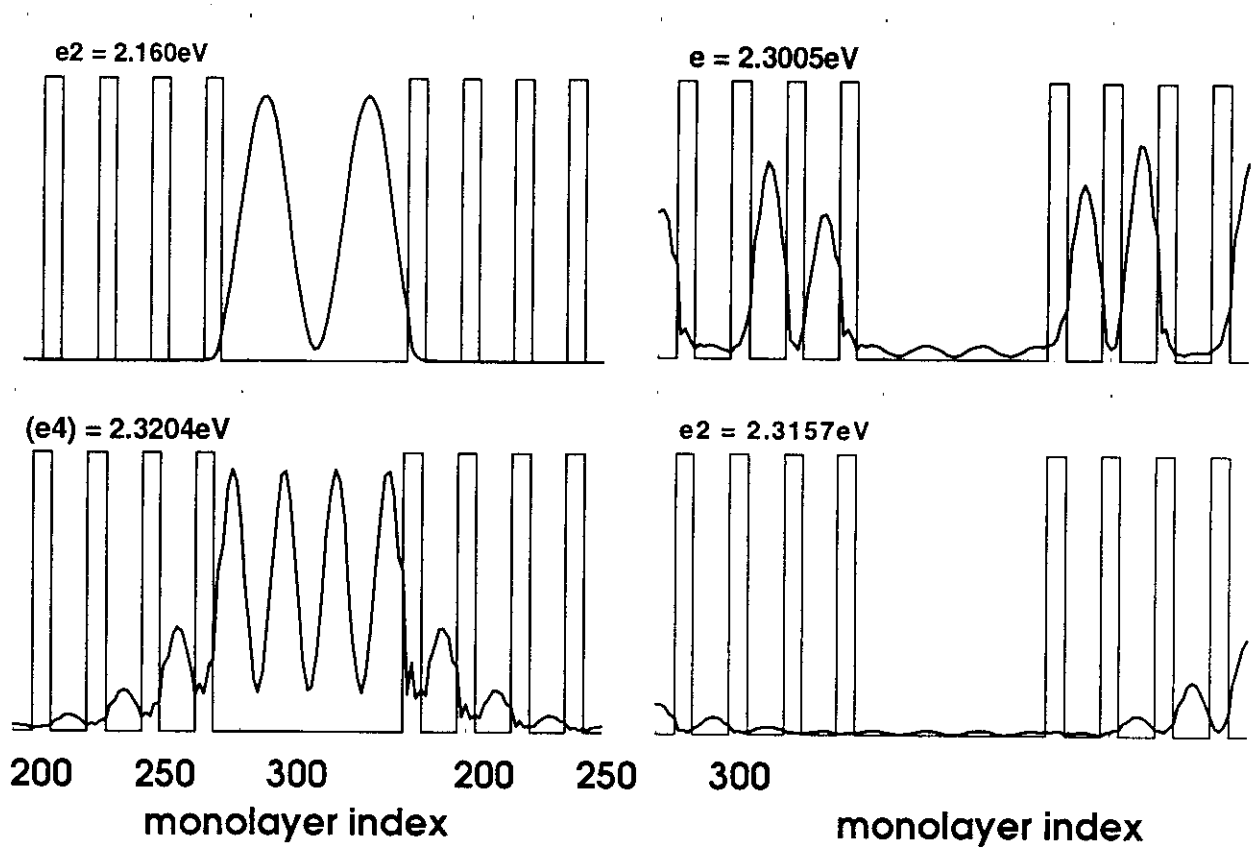

Fig.2 Spectral strengths for some states in the case of a GaAs QW of 42 monolayers embedded in an AlAs(4)/GaAs(8) SL

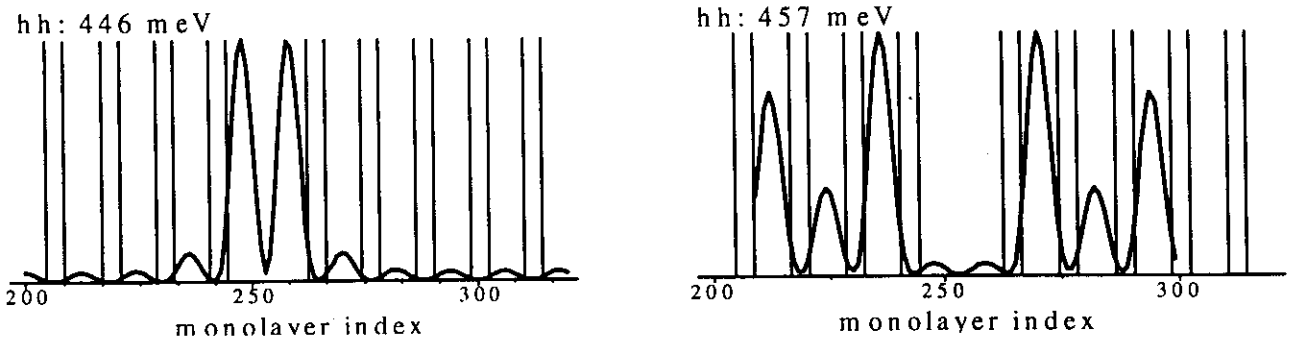

Fig.3 Spectral strengths for some states in the case of a GaAs QW of 18 monolayers embedded in an AlAs(4)/GaAs(8) SL

iv) *Conclusions*

The system containing a GaAs QW embedded in an AlAs/GaAs SL can be considered as formed by two components: SL and EW. The states which are isolated in energy show strong spatial localization in the embedded well. These states originate from the GaAs/AlAs quantum well and tend to conserve their localized character even when the AlAs barriers are replaced by a SL. On the other hand the states of the SL mini-bands, although slightly perturbed by the presence of the EW, are localized mainly in the SL. This situation changes when a state, originating from the GaAs/AlAs quantum well is close in energy or inside a SL mini-band. In that case one observes a significant delocalization of the mentioned state toward the SL. Besides, SL states penetrate in the EW.

II. Experimental studies by photoluminescence

i) *samples*

Planar structures containing GaAs QWs embedded in AlAs/GaAs SLs have been studied. They are grown in IMO, EPFL, Switzerland by MBE on (100) GaAs substrates. Two types of samples are used (Fig.4). Samples type A consist of a 50 A thick GaAs QW sandwiched between 26 and 20 periods of an AlAs(4)/GaAs(8). In samples type B the SL is the same, but they contain two EWs - one of 50A and one of 120A, the latter being below the former. In this case there are 5, 24 and 20 periods of SL situated bellow the 120A EW, between the EWs and above the 50A EW, respectively. . In both cases the cap layer is of AlGaAs with x equal to the mean Al content in the SL. Samples type B have a GaAs buffer layer of 400 nm between the substrate and the first SL.

ii) *Experimental set-up*

Photoluminescence (PL) spectra are measured at different temperatures and excitation densities.

The excitation was performed by an Ar ion laser or a He-Ne laser. The PL was detected using a double SPEX monochromator with a GaAs photomultiplier or a ccd - detector. The excitation densities have varied fro 0.5 to 3000 W/cm^2. (see Table 2)

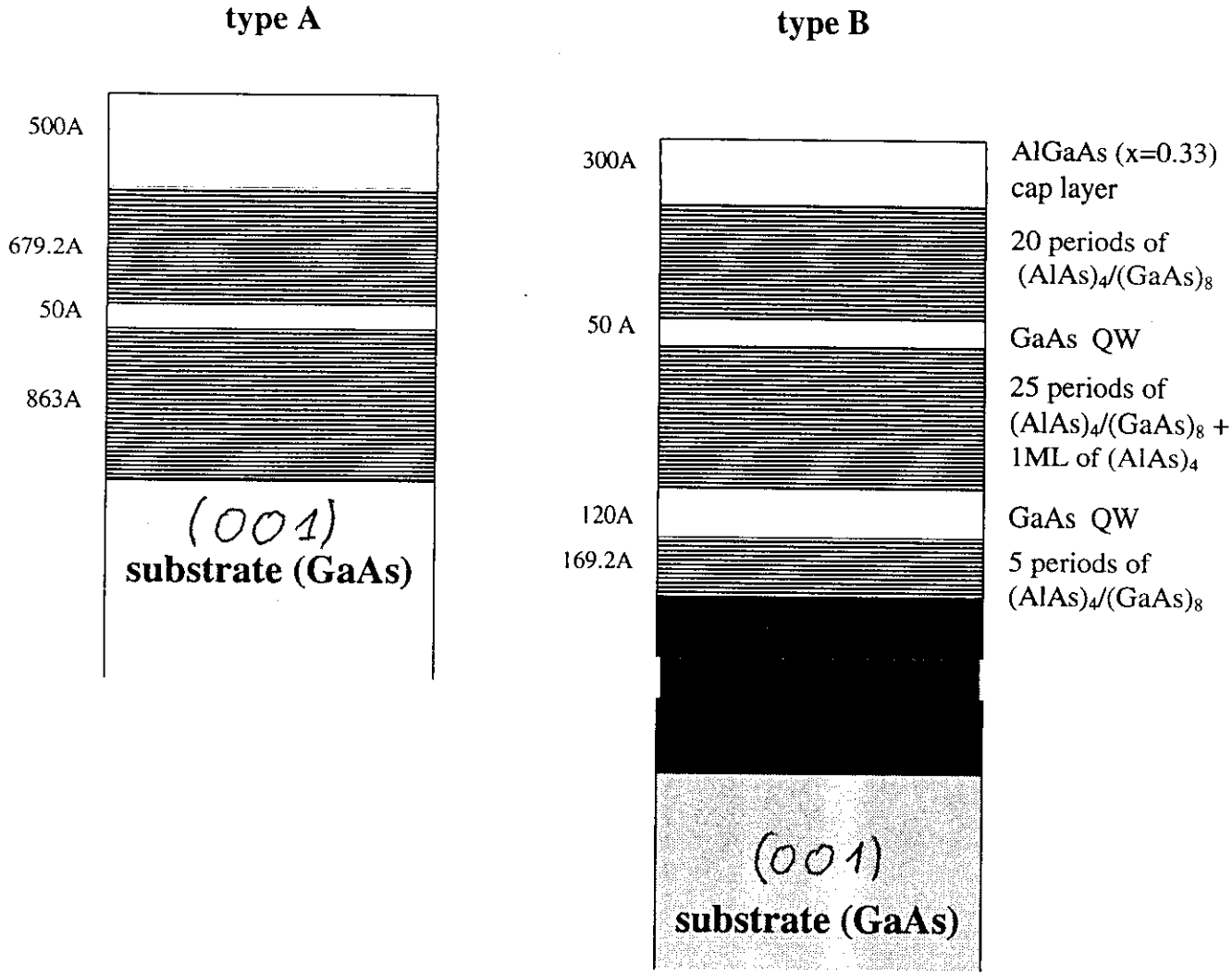

IMO, EPFL, Switzerland

Figure 4.

Table 2. Experimental details

T	excitation	detection Double SPEX (f=0.85m)	resolution
2-300K	He-Ne laser 632.8nm, 0.5-34 W/cm^2	GaAs photomultiplier	0.2 nm
2-300K	Ar -ion laser 501nm, 4-400 W/cm^2	ccd-line detector	0.025 nm
300K	Ar -ion laser 488nm, 300-3000 W/cm^2	GaAs photomultiplier	0.8 nm

iii) *Typical PL spectra*

Typical PL spectra at helium and room temperature are shown on Fig.5 and Fig.6 for sample type A and type B, respectively. The PL peaks are labeled P1 to P4 and S1 to S2. In samples type B one observes 2 new peaks (P1 and P2) in comparison with samples type A. With increasing the temperature S1 and S2 decrease rapidly ; the peaks P1 and P3 broaden and new peaks appear on their high energy side (P2 and P4, respectively) which at 300K look like shoulders. The energy distances of these high energy satellites (P2 and P4) to the corresponding peaks (P1 and P3) remain constant with the temperature - 12 and about 36 meV, respectively. Fig 7 represent a PL spectrum at 150K. P2 is clearly seen, while P4 just begin to appear like a shoulder. Fig.8 shows a PLE spectrum detected at the low-energy side of P3 in a sample type A. The nearest peak to P3 is at 43 meV.

v) *Excitonic character of the radiative recombination*

The character of the observed radiative recombination has been studied by analyzing the dependence of the photoluminescence (PL) intensity I_{PL} on the excitation density I_{exc}. It is shown that the following dependence takes place $I_{PL} \sim I_{exc}^{\alpha}$ [13,14]. Here the exponent α is :

α=1 for **excitonic** recombination (whether radiative or non-radiative recombination dominates),

α=2 for **free-carrier** recombination (assuming that non-radiative recombination dominates) and

$1 < \alpha < 2$ for the intermediate case where both free exciton and free carrier recombination take place.

From the slope of the dependence Lg(I_{PL}) versus Lg(I_{exc}) we have found α and so the character of the radiative recombination could be determined.

Figures 7 and 8 show the dependencies of the PL intensity on the excitation density for the peak P3 in a sample type A and for the peak P1 in a sample type B, respectively. The values of the coefficient α are also shown. They increase with the temperature because of the ionization of the excitonic levels. The results for α obtained in different samples are summarized in Table 3.

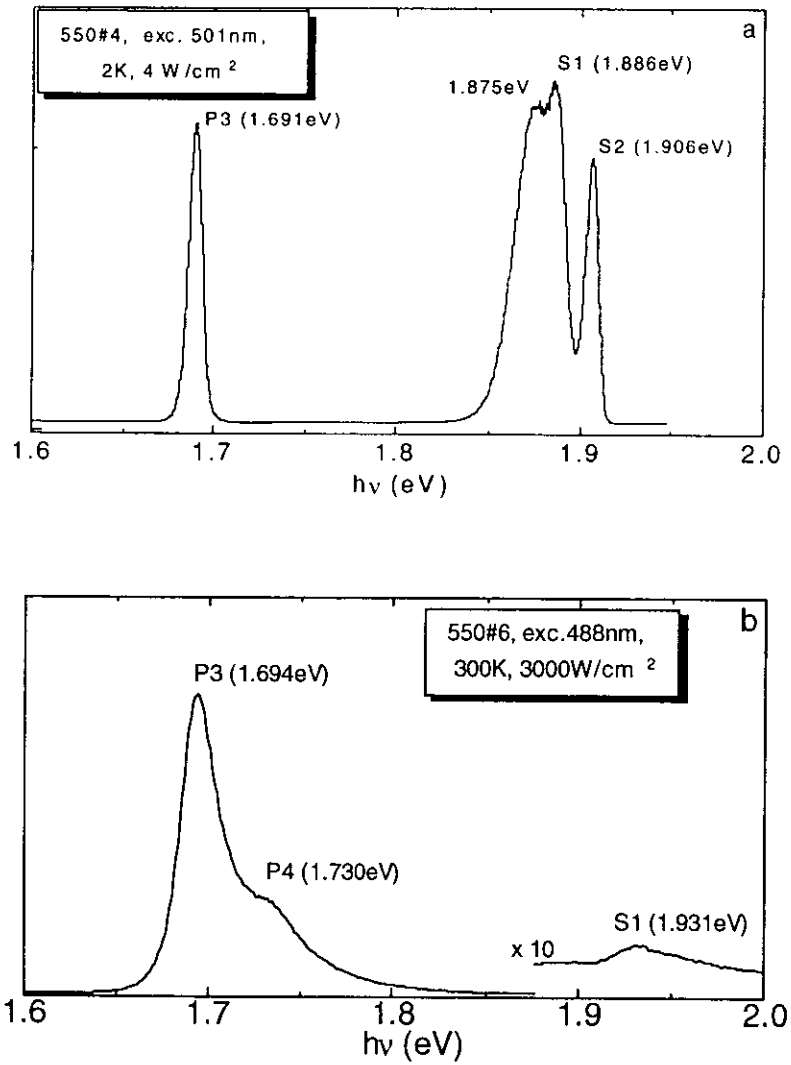

Fig. 5. Typical PL spectra of a sample type A at (a): 2K and (b): 300K

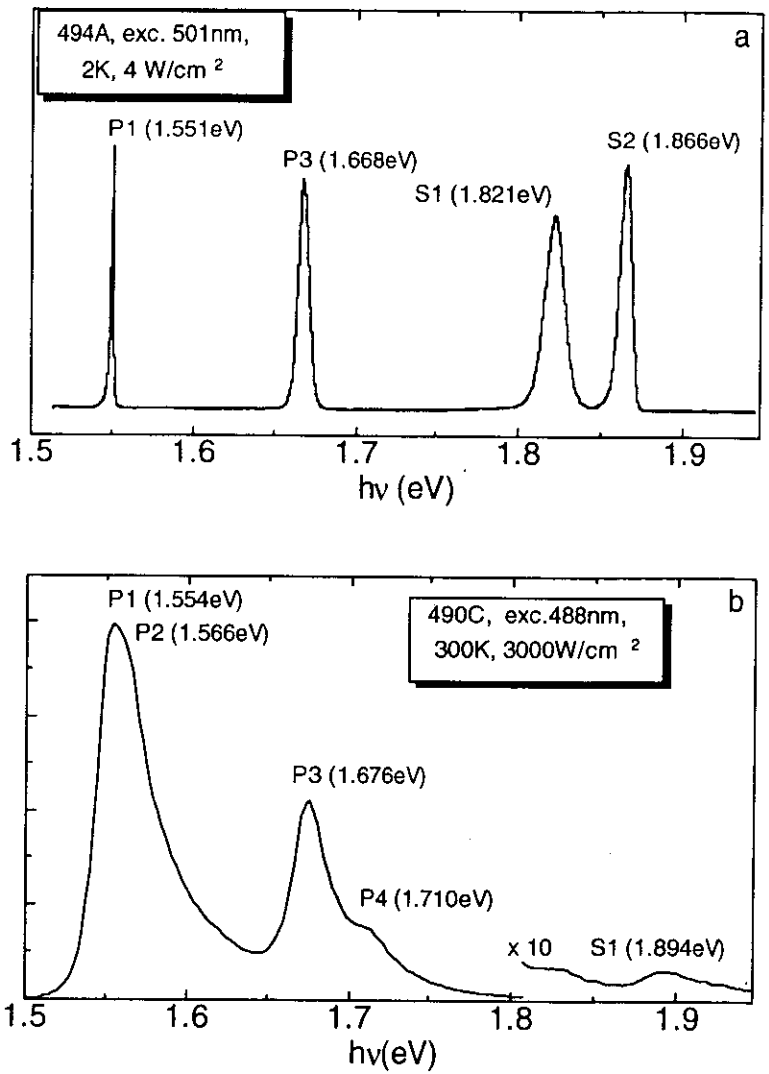

Fig. 6. Typical PL spectra of a sample type B at (a): 2K and (b): 300K

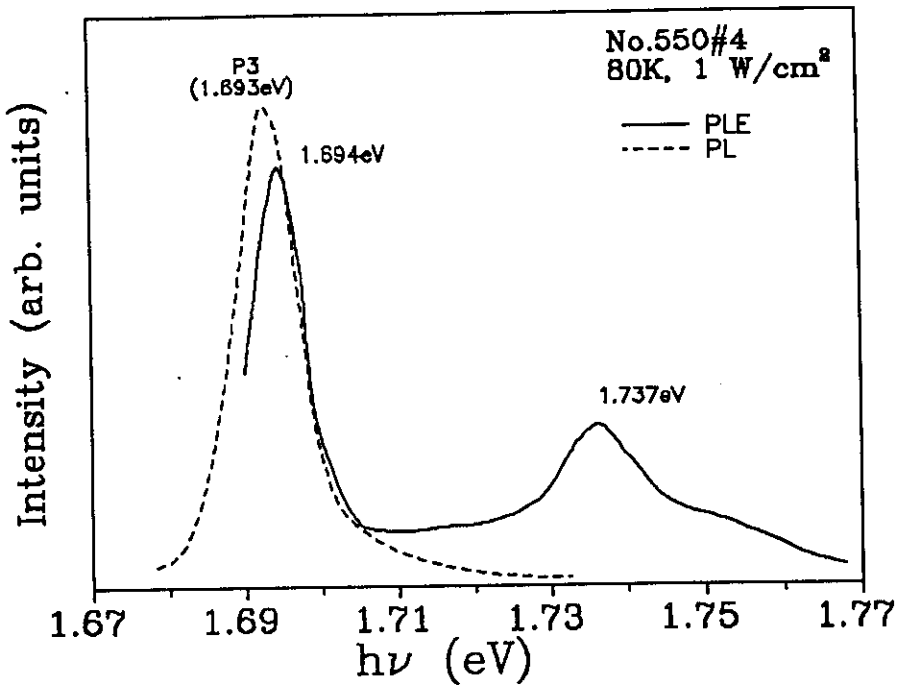
No.550#4
80K, 1 W/cm²
PLE
PL
P3
(1.693eV)
1.694eV
1.737eV
Intensity (arb. units)
1.67
1.69
1.71
1.73
1.75
1.77
hν (eV)

Fig. 8

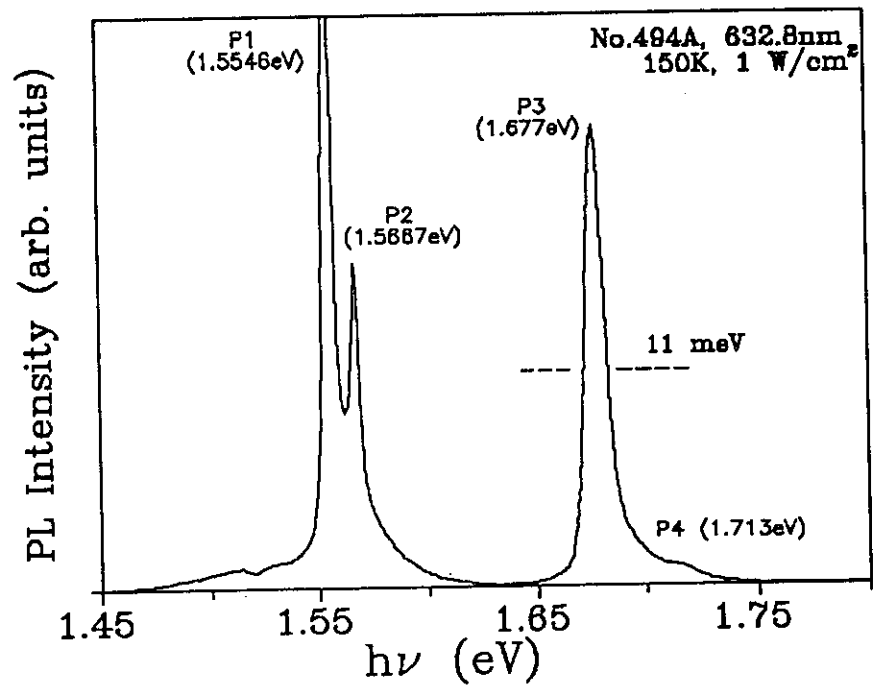
No.494A, 632.8nm
150K, 1 W/cm²
P1
(1.5546eV)
P2
(1.5687eV)
P3
(1.677eV)
11 meV
P4 (1.713eV)
PL Intensity (arb. units)
1.45
1.55
1.65
1.75
hν (eV)

Fig. 7

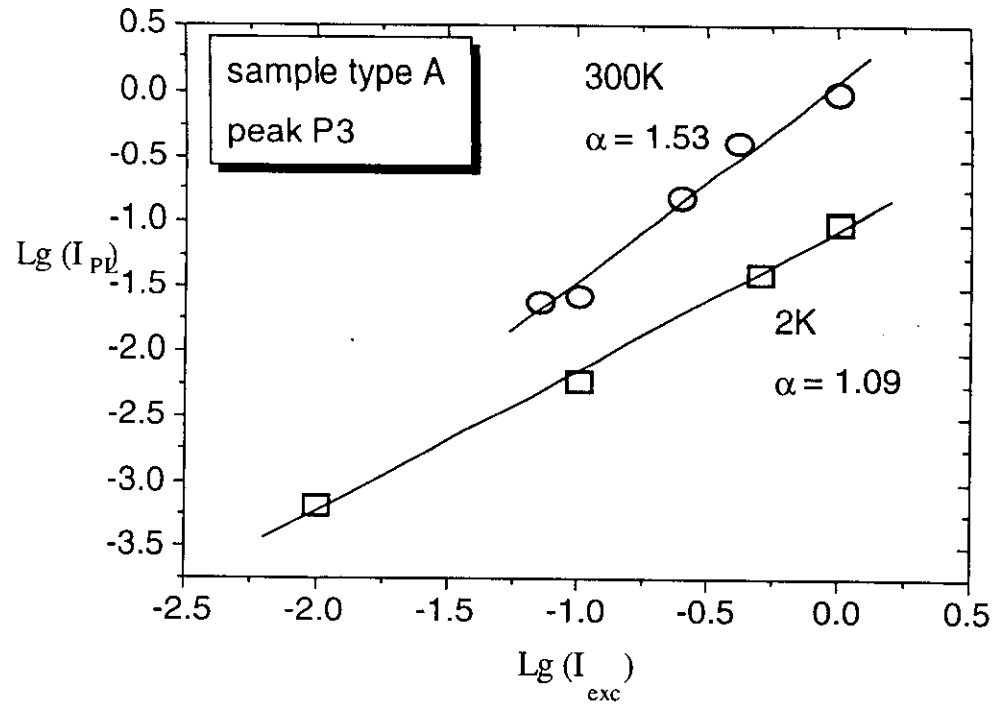

Fig.9. Excitation dependence of the photoluminescence intensity at 2K and 300K for a sample type A.

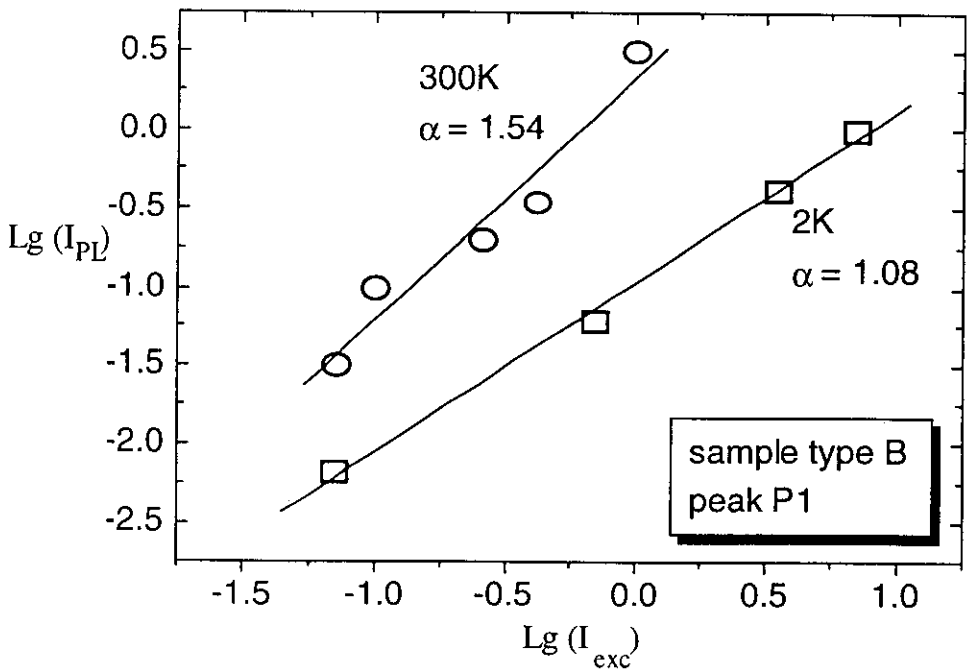

Fig.10. Excitation dependence of thephotoluminescence intensity at 2K and 300K for a sample type B.

At 2K α is very close to 1 for all the PL peaks observed which means that the radiative recombination occurs via excitons at low temperature. α remains below 2 up to 300K where it is around 1.5. This indicates that in the samples investigated the excitonic recombination remains dominant up to room temperature, where free carriers recombination also takes place.

Table 3. Results for the coefficient α obtained in different samples.
(A and B denote the sample type)

peak	2K	300K
P1	B: 1.08; 1.10; 1.29	B: 1.54; 1.81
P2	not seen	B: 1.21; 1.47
P3	A: 1.06 -1.18; B: 1.11 - 1.28	A: 1.53; B: 1.47; 1.67
P4	not seen	A: 1.41; B: 1.22; 1.44
S1	A: 1.08 - 1.10; B: 1.10 - 1.22	
S2	A: 0.88 - 0.96; B:1.0 - 1.18	

Conclusion : Excitonic recombination predominates at low temperature. This recombination remains dominant up to room temperature, where free carriers are also present.

IV. Identification of the PL peaks

Table 4 gives a comparison between calculated transition energies and the energy positions of the PL peaks observed in our samples.

As we have seen the peaks P1 and P3 exist only in the spectra type B (Figs.5,6). So, they are connected with the EW of 120 A. Indeed their energies fit well the calculated energies for the e1-hh1 and e1-lh1 transitions localized in this EW.

In the case of the 50A EW the situation is more complicated. There is nothing significant in the PL spectra in the range where falls the energies of the lowest transitions according to the calculations. One observes only small peaks which are hard to distinguish from the noise. This indicates that an other recombination channel is dominant.

The big peak P3 is present in the spectra of both type of samples, hence it does not originate from the 120A QW. Its energy position is away from the calculated transition energies corresponding to the lowest transitions in the EW of 50A and also from the transitions in the SL. So, the question of its origin is an open question.

i) *Table4. Transition energies (in meV) calculated by the ETB method . Comparison with photoluminescence peak positions.*

QW	Tran-sition	GaAs/AlGaAs Single QW			GaAs QW embedded in an AlAs(4)/GaAs(8) SL		
		E x=0.33	E x=1	E_{exc}	E	E - E_{exc}	PL peak (sample)
12 nm	e1-hh1	1570	1572	11	1572	1561	P1: 1552 (B)
	e1-lh1	1579	1581	13	1581	1568	P2: 1564 (B)
5 nm	e1-hh1	1624	1639	16	1639	1623	
	e1-lh1	1648	1673	21	1673	1662	
	e1-hh2				1701	1690	P3:
	e1-hh3				1702	1691	1691 (A)
	e1-hh4				1702.4	1691.4	1668 (B)
	e1-hh5			(11)	1703	1692	
	e1-hh6				1703.4	1692.4	1693 (A, PLE)
	e1-hh7				1704	1693	
	e1-lh2				1740	1729	P4:
	e1-lh3			(11)	1741	1730	1730 (A)
	e1-lh4				1742	1731	1710 (B)
	e1-lh5				1743	1732	1736 (A, PLE)
SL	e - hh			(5)	1803 - 1834	1798 - 1829	S1: 1822 (B) 1875,1887 (A)
SL	e - lh			(5)	1841 - 1904	1836 - 1899	S2: 1864 (B) 1907 (A)

E_{exc} =11 - 21 meV - for a SQW of GaAs /AlAs - from: G.Oelgart et al. Phys.Rev.B 49, 10456 1994)

E_{exc}=(11) meV - from temperature dependent PL

E_{exc}=(5) meV - excitons in a SL

Open questions:

1. Why the lowest transitions in the EW of 50 A are not seen in the PL spectrum?
2. The origin of the peaks P3, P4, S1, S2 = ?

Tentative explanation

1) P3, P4 - related to the EW (50A)

$$P3 \longleftrightarrow e1(EW) - hh\ (SL)$$

$$P4 \longleftrightarrow e1(EW) - lh\ (SL)$$

We have tentatively proposed an explanation as follows. The group of transitions between the first e-state localized in the EW of 50A and the lowest states from the SL hh mini-band have very close energies. They do not exist in the spectrum of the ideal SL, nor of the SQW. So, we suppose that this group of transitions gives rise to the large PL peak P3 in the PL.

The group of transitions which follows in energy (e1-lh2 to e1-lh5,...) is also specific for the EW. It includes hole states corresponding to the SL lh mini-band. Its separation from the hh mini-band is about 40 meV. This value corresponds well to the energy distance (43 meV) between the two peaks in the PLE spectrum of sample A detected at the lower energy side of P3 (Fig.8). This group of transitions corresponds in energy to the peak P4.

2) Hole localization in the SL

- due to - fluctuations in the width and in the potential of the SL layers,
  - interface defects
- disordered SL

To explain the origin of P3 we assume hh localization in the SL in the growth direction connected with unintentionally introduced interface imperfections and/or fluctuations in the thickness and in the potential of the SL layers. At low temperature this disorder can reduce considerably the hh transport to the EW The sharp doublet S1-S2 around 1.89 eV is typical for a SL with well-width fluctuations [15,16]. The energy distance between the peaks (21 meV in (A) and 43meV in (B)) roughly corresponds to 1 ML (A) and 2 MLs(B) fluctuations of a 8 MLs QW. So, we suppose that much more electrons than holes arrive to the 50A EW where they thermalize to the e1 state and recombine with hh from the SL thus giving rise to the peak P3. As to the 120A EW, it is very close to the buffer layer and the holes generated there can reach it and give rise to the peaks P1 and P2.

Disordered SLs have been investigated by *Deveau et al* [6] *Pavesi et al.* [16] , *Fujiwara et al.* [15] and other groups. The existence of a disorder in the SL can be proved as follows. We plot the ratio between the integrated PL intensities corresponding to the peaks P3 and S1 as a function of the inverse temperature. (Fig.9). Two activation energies can be obtained from this dependence: 0.1meV (in the range 2-15K) and 13 meV (in the range 30-80K). The first one corresponds to detrapping of weekly localized carriers. The second one - to more localized carriers. Its value (13meV) is to be compared with the calculated energy differences between the SL mini-band and the energy of a well enlarged by +1 or +2 monolayers (Table 5). For heavy holes it is between these two values. In the case of electrons and light holes 1 ML fluctuations are not sufficient to induce localization.

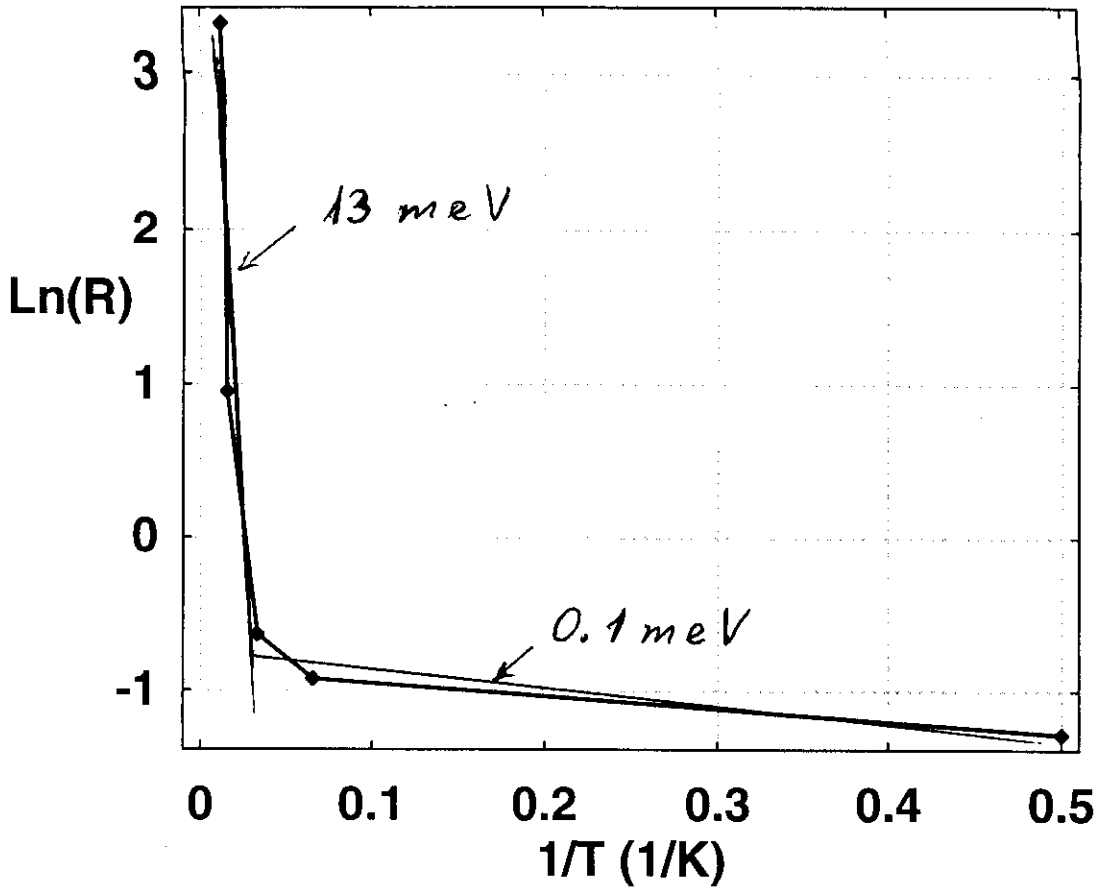

Figure 9. Temperature evolution of the peak ratio $R = \frac{I_{P3}}{I_{S1}} \infty \exp(-\frac{\Delta E}{kT})$

Table 5. Energy distance (in meV) between SL mini-band and an EW.
E<0 means that the state is inside the mini-band.

EW (MLs)	electrons	heavy holes	light holes
8 + 1	-1	8	-13
8 + 2	24	21	8

exp. : 13 meV , 60 meV

3) Non-radiative defects at the AlAs interfaces can also be considered to bleach the PL in the narrower EW where the wave function is more sensitive to the interfaces that in the larger EW.

4) e1(EW, 50A) ≈ e2(EW 120A); hh1(EW 50 A) ≈ hh2 (EW 120A)

The question about an interaction between the EWs has to be checked also.

5) S1 and S2 peaks

S1 ⟷ e-hh (SL)

S2 ⟷ e-lh (SL) or well width fluctuations 8-2=6,

S1 is more likely to be due to the SL hh exciton taking into account the calculated energies (see Table 4). As to S2 its origin is more unclear. Its separation from S1 correspond to the calculated hh-lh distance in the SL (see Table 4) and in the same time to a 2 ML fluctuation of the SL well (8+2).

It should be mentioned than a hh - lh mixing can be induced by the fluctuations in the well width in such short periods SLs.

V. Conclusions:

•The ETB calculations of the electronic structure of GaAs QW embedded in AlAs/GaAs SLs have shown **an interaction** between the two components of the system. It occurs under certain conditions and modifies the electronic structure of both QW and SL.

•The PL measurements revealed optical transitions which do not exist in the spectrum of a single QW, nor of an ideal SL. It is found that some of these new transitions are dominant in the emission spectrum of the structures considered.

Acknowledgments:

- We are grateful to Prof. F.K.Reinhart and D.Martin from EPFL for supplying the samples.
- This work was supported by the Bulgarian National Science Fund.

References:

1. Weisbuch, and B. Vinter, *Quantum Well Structures. Fundamentals and Applications*, Academic Press, Inc., San Diego and New York, 1991.
2. R.Kucharczyk and M.Steslicka, *Solid State Commun.* **81**.(1992), 557.
3. V.Donchev, I.Ivanov, and K.Germanova, in: *Heterostructure Epitaxy and Devices* (eds J.Novak and. A.Schlachetzki), NATO ASI Series, 3. High Technology - vol. 11, Kluwer Academic Publishers, Dordrecht, 1996, .83
4. H.Sakaki, M.Tsuchiya, and J.Yshino,. *Appl.Phys.Lett.* **47** (1985), 295.
5. P.Blood, in: *Physics and Technology of Heterostructure Devices,* (eds. D.V.Morgan and R.h.Williams), Peter Perigrinus, 1991, Chap.7, 231
6. B.Deveaud, J.Shah, T.C.Damen, B.Lambert, A.Chomette, and A.Regreny, *IEEE J. Quantum Electronics* **24** (1988), 1641.
7. P.Vogl, H.P.Hjalmarson and J.D.Dow, J.Phys.Chem.Solids **44**, 365 (1983)
8. C.Priester, G. Allan and M.Lannoo, Phys.Rev. B **37**, 8519 (1988)
9. F.Garcia-Moliner and V.R.Velasko, Theory of Single and Multiple Interfaces. The Method of Surface Green Function Matching (World Scientific, Singapore, 1993).
10. S.Vlaev, V.R.Velasco and F.G.Moliner, Phys.Rev. B **49**, 11222 (1994); *Phys.Rev.B* **50,** 4577 (1994) ibid. **51**, 7321 (1995); ibid. **52**, 13784 (1995)
11. S.Vlaev, in: M.Balkanski and I.Yanchev (eds), Fabrication, Properties and Appl.of Low-Dimensional. Semiconductors, Kluwer Academic Publishers, Dordecht 1995, p.141.
12. A.Aldea, S.Vlaev, G.Monsivais, F.Garcia-Moliner and V.R. Velasco, J.Phys.: Condens. Matter, **8**, 7733 (1996).
13. Xu.Zhongying et al. *Solid State Commun.* **61** (1987), 707.
14. J.E.Fouquet and A.E.Siegman, *Appl.Phys.Lett.* **46** (1984), 280.
15. Fujiwara, K., Tsukada, N. and Nakayama, T., Linear polarization effects on photoluminescence properties of GaAs/AlAs quantum well heterostructures, Solid State Commun. **69**, 63-66 (1989).
16. Pavesi, L., Tuncel, E., Zimmermann, B. and Reinhart, F.K., Photoluminescence of disorder-induced localized states in GaAs/AlGaAs superlattices, Phys.Rev. B **39**, 7788-7795 (1989).